Two-Way Optical Frequency Comparisons at $5 \cdot 10^{-21}$ relative stability Over 100-km Telecommunication Network Fibers

Anthony Bercy,[1,2] Fabio Stefani,[2] Olivier Lopez,[1] Christian Chardonnet,[1] Paul-Eric Pottie,[2,*] and Anne Amy-Klein[1]

[1] *Laboratoire de Physique des Lasers, Université Paris 13, Sorbonne Paris Cité, CNRS, 99 Avenue Jean-Baptiste Clément, 93430 Villetaneuse, France*

[2] *Laboratoire National de Métrologie et d'Essais-Systèmes de Référence Temps-Espace, UMR 8630 Observatoire de Paris, CNRS, UPMC, 61 Avenue de l'Observatoire, 75014 Paris, France*

(Dated: October 17, 2014)

By using two-way frequency transfer, we implement a real-time frequency comparison over a uni-directional telecommunication network of 100 km using a pair of parallel fibers with simultaneous digital data transfer. The relative frequency stability is 10^{-15} at 1-s integration time and reaches $2 \cdot 10^{-17}$ at 40 000 s, three orders of magnitude below the one way fiber instability. We also demonstrate ultra-high resolution comparison of optical frequencies with a bi-directional scheme using a single fiber. We show that the relative stability at 1-s integration time is $7 \cdot 10^{-18}$ and scales down to $5 \cdot 10^{-21}$. The same level of performance is reached when an optical link is implemented with an active compensation of the fiber noise. The fractional uncertainty of the frequency comparisons was evaluated for the best case to $2 \cdot 10^{-20}$. These results open the way to accurate and high resolution frequency comparison of optical clocks over intercontinental fiber networks.

PACS numbers: 06.20.fb, 06.30.Ft, 42.62.Eh

High resolution time and frequency transfer between remote locations are of major interest for many applications, such as tests of general relativity and temporal variation of fundamental constants, future redefinition of the second, relativistic geodesy and navigation (see [1] and references herein). It is usually performed through satellite-based time and frequency transfer but with performance now insufficient for state-of-the-art optical clocks and laser oscillators [2–4]. As a very promising alternative, optical fiber links are intensively studied by several groups for frequency transfer for a decade [5–7]. They demonstrate impressive results far beyond the GPS capabilities on distances up to 1840 km with bi-directional dedicated fibers [8]. Our groups extended the technique of optical link to active telecommunication fiber networks by inserting Optical Add-Drop multiplexers (OADM) in every amplification sites and network nodes. Bi-directional frequency transfer was enabled on one 100-GHz dedicated channel, in parallel with uni-directional data traffic over all the other channels [9]. This technique proved to be very efficient for ultra-stable time and frequency transfer on a continental scale [10]. It gives the possibility to disseminate a frequency standard to a wide number of laboratories, for high-resolution spectroscopy, remote laser stabilization, and any high precision measurements.

If one focus on optical frequency comparisons, and let the frequency transfer aside, the set up can be drastically simplified with two-way method [11]. At each end of the fiber link, a laser is sent to the other end and one detects the frequency difference between the local laser and the remote laser. Assuming that the propagation frequency noise is equal for the two directions of propagation, one can efficiently reject the propagation contributions by synchronizing and post-processing the data, simply subtracting and dividing by two the two data sets recorded at each end. The in-field implementation of the two-way method requires two ultra-stable lasers at each end, and an accurate control of their frequency drifts. This can be done actively by locking the laser frequency to an atomic clock or a Maser, or passively by time stamping the data of the frequency measurements in both laboratories [12].Two-way frequency comparison was recently demonstrated over a 47-km loop in an urban link using a Sagnac interferometer [13]. But the latter imposes the two ends to be in the same place. We consider in this paper two alternative two-way schemes which can be practically implemented between distant laboratories and we demonstrate them over a 100-km urban link. One scheme uses a single fiber through which the light is propagated in both directions (from here referred to as two-way bi-directional or 2way-B). It exhibits a very low instability, thanks to the very good rejection of the fiber noise. The other one uses two parallel fibers, each fiber transmitting the light in a single direction (referred to as two-way uni-directional or 2way-U) as first proposed by [14]. Despite its higher instability, this uni-directional scheme outperforms satellite comparison techniques for short averaging time. Moreover it opens the way to frequency comparisons over telecommunication network with minimal modification of the network backbone.

The paper is organized as follows : we describe first the two schemes of two-way frequency comparisons we have implemented. Second we present the experimental results and the extrapolation to long haul terrestrial and submarine links of uni-directionnal two-way frequency comparisons.

In order to demonstrate in real conditions two-way

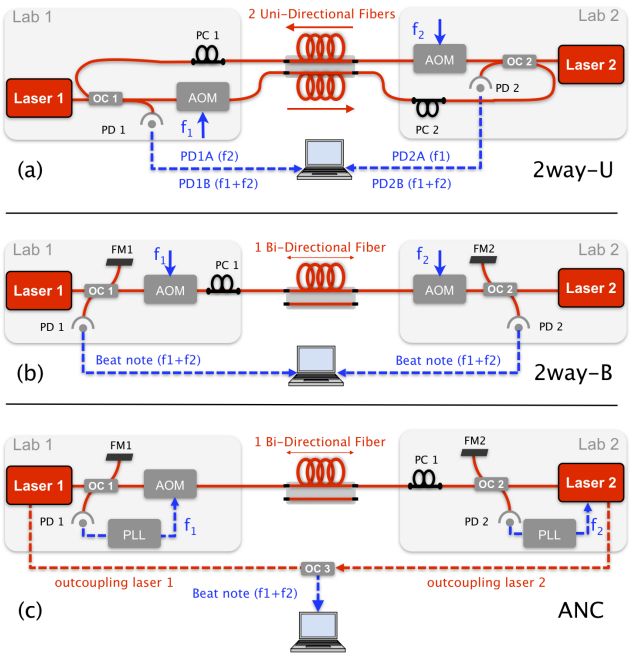

FIG. 1. Experimental set ups for frequency comparison: a) two-way uni-directional b) two-way bi-directional c) active noise compensated link. AOM : Acousto-Optic Modulator. PC : Polarization Controller. FM : Faraday Mirror. OC : Optical Coupler. PD : Photo-Diode PLL : Phase Lock Loop.

frequency comparison and to asset its performances, we used a pair of optical fibers forming two parallel loops of 100 km in Paris area (see supplementary materials [15] Section 1). The loop starts and ends at Laboratoire de Physique des Lasers. However we use two detection set-ups (one at each end), to make it usable for two distant laboratories, as detailed below.

We have first implemented a two-way method using two fibers and uni-directional propagation. This configuration can be straightforward employed on telecommunication networks which are operated this way. The set up is sketched on Fig. 1a. The left to right and right to left counter-propagating optical signals are propagating into two uni-directional fibers. The frequency of the two lasers located at each end are shifted with two Acousto-Optics Modulators (AOM) at frequencies f_1 and f_2, one on each fiber, in order to distinguish the useful signals from parasitic back-reflections. At each end, a Michelson-type interferometer is implemented, instead of the circulators of the first proposal [14]. This new configuration enables to detect two beat notes on the two photodiodes PD1 and PD2 at each end : the beat note between the local and remote lasers, of frequency f_1 or f_2, labelled as A, and the beat note between the local laser with itself after a round trip in both fibers successively, of frequency $f_1 + f_2$, labelled as B. The beat notes are optimized with two polarization controllers. After amplification and filtering, the beat notes are simultaneously recorded with frequency counters with a gate time of 1 s (see supplementary materials [15] Section 1).

Let us consider a simplified, steady state model of the two-way phase detected in that configuration. One can write the beat note signals detected by the photodiodes PD1 and PD2 as follows :

$$\begin{cases} \mathrm{PD1}_A = (\Phi_2 + \Phi_{21}) - \Phi_1 & \text{at frequency } f_2 \\ \mathrm{PD1}_B = (\Phi_{12} + \Phi_{21}) & \text{at frequency } f_1 + f_2 \\ \mathrm{PD2}_A = (\Phi_1 + \Phi_{12}) - \Phi_2 & \text{at frequency } f_1 \\ \mathrm{PD2}_B = (\Phi_{12} + \Phi_{21}) & \text{at frequency } f_1 + f_2 \end{cases} \quad (1)$$

where Φ_1 and Φ_2 are the phase noises associated to Laser 1 and Laser 2, and Φ_{12} and Φ_{21} the noises added by the two fibers respectively (independent of the lasers at first order). It can be easily demonstrated that, for any realistic amount of fiber attenuation, the successive loops of light signals are not perturbing the considered measurements.

Combining the signals labelled as A in Eq. 1 in post-processing gives :

$$(-\mathrm{PD1}_A + \mathrm{PD2}_A)/2 = (\Phi_1 - \Phi_2) + (\Phi_{12} - \Phi_{21})/2 \quad (2)$$

This signal will be referred to as remote two-way uni-directionnal. Under the assumption that $\Phi_{12} = \Phi_{21}$, one finds the standard two-way noise rejection, as the fiber noise cancels out and only the laser's phase difference remains. Assuming that the phase noise of both fibers is partly correlated in this set-up, one expects a partial noise cancellation for a frequency comparison. The same results can be obtained by combining the two beat notes of the same photodiode. For instance on PD 1 one has :

$$-\mathrm{PD1}_A + \mathrm{PD1}_B/2 = (\Phi_1 - \Phi_2) + (\Phi_{12} - \Phi_{21})/2 \quad (3)$$

and similarly on PD 2. This approach, that we called "local two-way", allows us to process the noise rejection at each distant laboratory, using only data acquired locally. It avoids the necessity to exchange and synchronize data between distant sites to remove the propagation noise. When using the same laser at both ends, the term $(\Phi_1 - \Phi_2)$ vanished in the above equations and one is only sensitive to the residual uncorrelated fiber's noise.

To reject this uncorrelated fiber's noise, one single fiber has to be used for the two counter propagating signals. In order to study this noise rejection, we tested a two-way bi-directional configuration (see Fig. 1b). The set-up is similar to that of the 2way-U, with two AOMs at frequencies f_1 and f_2 and two Michelson-type interferometers, one at each end of the single fiber. A single polarization controller is used to optimize the beat notes. With this set-up we detect on each photodiode a single beat-note between the local and remote lasers, at frequency $f_1 + f_2$. After detection, amplification and filtering, the two end's beat notes are simultaneously counted and processed to obtain the optical frequency comparison, as with the 2way-U set-up.

Following the general approach of [5], we can derive the residual expected noise of this bi-directional two-way set-up [13]. Its origin is similar to that of the delay-unsuppressed noise in a noise compensated link. The total one-way phase perturbation Φ_{12} (respectively Φ_{21}) arising for the signal propagating from Lab 1 to Lab 2 (see Fig. 1)(respectively from Lab 2 to Lab 1) reads: $\Phi_{12}(t) = \int_0^L \delta\varphi\left(z, t - \frac{L-z}{v}\right) dz$ and $\Phi_{21}(t) = \int_0^L \delta\varphi\left(z, t - z/v\right) dz$, where v is the light celerity in the fiber, L the length of the loop, and $\delta\varphi$ the phase perturbation per unit of length at coordinate z at time t. For slow variation of the phase noise per unit of length compared to the round-trip time, the two-way phase $\Phi_{\mathrm{tw}(t)} = 1/2(\Phi_{12}(t) - \Phi_{21}(t))$ can be derived at first-order as:

$$\Phi_{\mathrm{tw}}(t) = \frac{1}{2}\int_0^L \frac{\partial\delta\varphi(z,t)}{\partial t} \cdot \left(\frac{2z-L}{v}\right) dz \qquad (4)$$

The two-way phase noise power spectral density (PSD) of this signal is calculated as the Fourier transform of its autocorrelation function, $R_{\mathrm{tw}}(\tau) = \overline{\Phi_{\mathrm{tw}}(t)\Phi_{\mathrm{tw}}(t+\tau)}$ [16]. Assuming that the fiber noise per unit of length is uncorrelated in position and has constant statistical properties over z [16], one obtains:

$$S_{\Phi_{\mathrm{tw}}}(\omega) = S_{\Phi_{12}}(\omega) \cdot \frac{(2\pi f \cdot L/v)^2}{12} \qquad (5)$$

where $S_{\Phi_{12}}(\omega)$ is the one-way phase noise PSD expressed in $\mathrm{rad}^2/\mathrm{Hz}$. This formula is very similar to that obtained for an optical link with active noise compensation, but with a factor $1/12$ instead of $1/3$, since the two-way phase is half of the difference between the one-way phase signals [5, 13]. It gives an additional rejection factor of $1/4$ for the two-way bi-directional set-up.

In order to check this statement, we set up on the same 100-km fiber loop an active noise compensated link, (see Fig. 1c) referred to as *ANC* later on [17], and recorded the beat note between the two ends of the link at the same frequency $f_1 + f_2$. A noticeable change is that the fiber laser is then phase locked to an ultra-stable laser, itself locked to an ultra stable cavity, transferred from SYRTE to LPL on a 43-km long dedicated fiber [18].

We asset the ultimate performances of the two-way set-ups by injecting both ends with a single fiber laser. For each set-up, the two interferometers are hosted in a single, thermally controlled box. They are carefully designed, so that most of the interferometer noise is rejected [19].

We first derive the relative frequency stability of the frequency comparisons, expressed as the modified Allan deviation (MDEV) [20]. Fig. 2 displays these stabilities for the one-way fiber noise (green up triangles, a), the remote 2way-U (blue rounds, b), the local 2way-U (red squares, c), and the 2way-B (black diamonds, e). For both configurations, we did not suppress any point

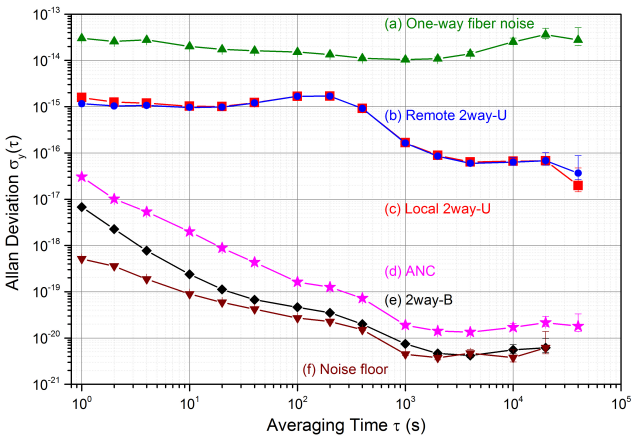

FIG. 2. Fractional frequency instability derived from data recorded with Λ-counter and expressed as the modified Allan deviation for (a) One-way fiber noise (b) Two-way uni-directional as reconstructed from data recorded at the 2 ends (c) Local two-way uni-directional (d) Active noise compensated link (e) Two-way bi-directional. (f) Two-way bi-directional noise floor. The other noise floors are similar and are not shown for sake of clarity.

from the data sets. The local two-way uni-directional stability is as low as 10^{-15} at 1 s integration time and reaches $2 \cdot 10^{-17}$ at 40 000 s. The remote 2way-U has almost the same performance. This result demonstrates the excellent capabilities of 2way-U for frequency comparison of the best atomic fountain clocks. This level of performance is indeed already far beyond the most advanced GPS and Two-Way Carrier Phase capabilities [4]. The two-way bi-directional stability is as low as $7 \cdot 10^{-18}$ at 1 s and reaches $5 \cdot 10^{-21}$ at 4 000 s, which is one the best frequency comparison stability reported so far in a very noisy urban environment. For averaging times longer than 100 s, it is limited by the noise floor (brown down triangles, f). We also plot on Fig. 2 the stability of an ANC link using the same fiber loop of 100 km (pink stars, d). The 2way-B relative stability is about four times below the one of the ANC set-up, which is more than expected.

To further investigate the noise rejection of the three set-up sketched on Fig. 1, we plot on Fig. 3 their phase noise Power Spectral Densities (PSD). The measurements were done using a frequency counter with a gate time of 1 ms and Π-type operation. Frequency data were converted to phase data. Referring to Eq. 5 and [5], the ANC PSD was scaled by a factor 1/4 (*i.e.*-6 dB) in order to make the comparison with the 2-way PSDs easier. The two upper curves of Fig. 3 are the noise PSDs of the one-way (orange curve, a) and the free-running fiber noise (green curve, b), the latter being measured with the ANC set-up using a frequency-stabilized laser. The one-way PSD exhibits an excess noise compared to the free-running fiber noise for $f < 5 \cdot 10^{-1}$ Hz which

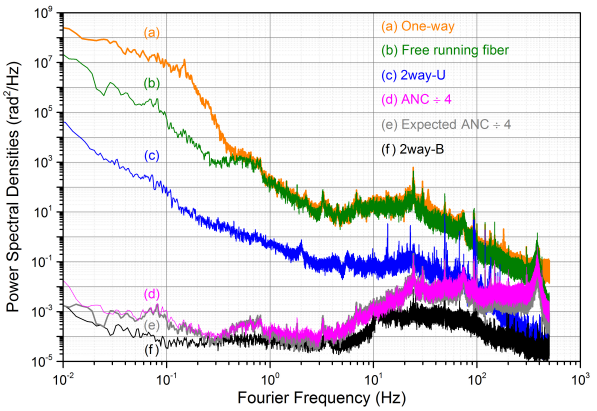

FIG. 3. Phase noise PSD for the three set-up of Fig. 1 1s: (a) One-way, (b) Free running fiber noise for the ANC set up (c) Two-way uni-directional, where real-time and post-processed overlapped themselves , (d) Active noise compensation (÷4), (e) Expected ANC (÷4) (f) Two-way bi-directional.

is due to the noise of the un-stabilized laser used for the two-way set-ups. This common noise source for the two counter propagating signals is well rejected with the two-way set-ups. The 2way-U PSD (blue curve, c) is about two orders of magnitude below the free-running fiber noise, demonstrating a significant rejection of the propagation noise. The 2way-B PSD is at a very low level of around $6 \cdot 10^{-5}$ rad^2/Hz between 0.1 Hz and 60 Hz. Although showing a similar behavior, it is below the scaled ANC PSD (pink curve, d), when both curves were expected to coincide from the theoretical prediction. We checked that the ANC PSD was overlapping with the expected unsuppressed noise (grey curve, e) calculated from the free-running fiber noise [5, 16]. Thus the discrepancy between the ANC and 2-way-B noise PSDs may result from an overcorrection in the 2-way-B set-up. This rejection anomaly shows that the assumptions we made on Eq. 4, and on homogeneous noise and uncorrelated noise in position, are violated at some point. In an urban area network, we are indeed observing greater acoustic noise compare to optical links deployed in field. Further investigations are needed on the noise correlation properties in such two-way bi-directional set up.

We now extrapolate our result on 2way-U frequency comparison to a 800-km link, connecting Paris to London for instance. We are expecting that the stability is limited by the uncommon fiber noise, which we assume homogeneous with a deviation scaling as $\sqrt{L}$. We thus calculate a MDEV of $4 \cdot 10^{-15}$ at 1 s and $9 \cdot 10^{-17}$ at 30 000 s integration time. When considering a transatlantic link, one has to take into account that the noise deviation of a submarine link is about 10 times smaller [21]. For a link constituted of 6 500-km submarine link and 1 000-km terrestrial link, we obtained an expected MDEV of $5 \cdot 10^{-15}$ at 1 s and $1 \cdot 10^{-16}$ at 30 000 s integration time, dominated by the terrestrial noise. We checked that the delay unsuppressed noise, scaling as $L^{3/2}$, is below the uni-directional noise. This extrapolation must be confirmed with realistic data on fiber losses and on submarine amplifier's gain. The cumulative spontaneous emission of the optical amplifiers (up to 75) can be the limiting factor of such a method.

Finally we evaluate the accuracy of the frequency comparison. We calculate the mean value of the beat note frequencies recorded with a Π-type counter and we set the statistical fractional uncertainty of the frequency comparison as the long-term overlapping Allan deviation (see supplementary materials [15] Section 2). For the bi-directional set up, with the set of 138 000 data of 1 s of Fig. 2, we obtained a mean offset frequency of $7 \cdot 10^{-21}$ and a statistical fractional uncertainty of $2 \cdot 10^{-20}$. For the two-way uni-directional, using 160 000 data of 1 s of the remote comparison, we find a relative mean offset frequency of $8 \cdot 10^{-18}$ with a statistical fractional uncertainty of $6.5 \cdot 10^{-17}$ at 40 000 s integration time. This demonstrates that the frequency comparison shows no deviation to the expected value.

We have demonstrated two set-ups able to compare optical frequencies between two distant laboratories at ultra-high resolution and short averaging time on a 100-km telecommunication network. The first set-up uses two fibers for each propagation way and comply with uni-directional amplifiers used in telecommunication networks. It can be easily implemented over telecommunication network under operation, as long as the switches and routers are bypassed. We demonstrated a frequency comparison with a relative frequency stability of $2 \cdot 10^{-17}$ at 40 000 s integration time in 1 Hz bandwidth. This two-way uni-directional method gives the possibility to perform measurements *in situ* and in real-time. It opens the way to intercontinental clocks comparison with fiber links in parallel with data traffic at a level of resolution and accuracy competitive with the most advanced satellite techniques and with much shorter integration time. The second two-way set-up uses bi-directional frequency transfer in a single fiber. It gives the possibility to perform accurate and high-resolution frequency comparison with simple electronics, with outstanding relative stability of $5 \cdot 10^{-21}$ at 4 000 s integration time.

The authors thank Giorgio Santarelli for helpful and stimulating discussions. They also thank Emilie Camisard, Thierry Bono and Patrick Donath at the GIP Renater, and François Biraben, François Nez and Saïda Guellati-Khelifa at Laboratoire Kastler-Brossel, and Christian Hascoet and his team of Information Technologies Department at Pierre-et-Marie-Curie University (UPMC) for giving the opportunity to use the different spans of the fiber's loop.

This work is supported by the European Metrology Research Programme (EMRP) under SIB-02 NEAT-FT. The EMRP is jointly funded by the EMRP partici-

pating countries within EURAMET and the European Union. This work is supported by the E.U. under GN3+, the Labex FIRST-TF, the french spatial agency CNES, IFRAF-Conseil Régional Ile-de-France and Agence Nationale de la Recherche (ANR BLANC 2011-BS04-009-01).

* paul-eric.pottie@obspm.fr

[1] F. R. Giorgetta, W. C. Swann, L. C. Sinclair, E. Baumann, I. Coddington, and N. R. Newbury, Nat. Photon. **7**, 434 (2013), doi:10.1038/nphoton.2013.69.

[2] B. J. Bloom, T. L. Nicholson, J. R. Williams, S. L. Campbell, M. Bishof, X. Zhang, W. Zhang, S. L. Bromley, and J. Ye, Nature **506**, 71 (2014), doi:10.1038/nature12941.

[3] T. Kessler, C. Hagemann, C. Grebing, T. Legero, U. Sterr, F. Riehle, M. J. Martin, L. Chen, and J. Ye, Nat. Photon. **6**, 687 (2012), doi:10.1038/nphoton.2012.217.

[4] M. Fujieda, D. Piester, T. Gotoh, J. Becker, M. Aida, and A. Bauch, Metrologia **51**, 253 (2014), doi:10.1088/0026-1394/51/3/253.

[5] N. R. Newbury, P. A. Williams, and W. C. Swann, Opt. Lett. **32**, 3056 (2007), http://www.opticsinfobase.org/ol/abstract.cfm?URI=ol-32-21-3056.

[6] K. Predehl, G. Grosche, S. M. F. Raupach, S. Droste, O. Terra, J. Alnis, T. Legero, T. W. Hänsch, T. Udem, R. Holzwarth, and H. Schnatz, Science **336**, 441 (2012), doi: 10.1126/science.1218442.

[7] O. Lopez, A. Haboucha, B. Chanteau, C. Chardonnet, A. Amy-Klein, and G. Santarelli, Opt. Express **20**, 23518 (2012), http://dx.doi.org/10.1364/OE.20.023518.

[8] S. Droste, F. Ozimek, T. Udem, K. Predehl, T. W. Hänsch, H. Schnatz, G. Grosche, and R. Holzwarth, Phys. Rev. Lett. **111**, 110801 (2013).

[9] F. Kéfélian, O. Lopez, H. Jiang, C. Chardonnet, A. Amy-Klein, and G. Santarelli, Opt. Lett. **34**, 1573 (2009).

[10] O. Lopez, A. Kanj, P.-E. Pottie, D. Rovera, J. Achkar, C. Chardonnet, A. Amy-Klein, and G. Santarelli, Applied Physics B **110**, 3 (2013).

[11] D. W. Hanson, **Proc. of 43rd Annual Frequency Control Symposium** (1989).

[12] G. G. S. D. S.M.F. Raupach, H. Schnatz, Proc. of European Frequency and Time Forum, (2012), dOI: 10.1109/EFTF.2012.6502357.

[13] C. E. Calosso, E. Bertacco, D. Calonico, C. Clivati, G. A. Costanzo, M. Frittelli, F. Levi, A. Mura, and A. Godone, Opt. Lett. **39**, 1177 (2014), http://dx.doi.org/10.1364/OL.39.001177.

[14] P. A. Williams, W. C. Swann, and N. R. Newbury, J. Opt. Soc. Am. B **25**, 1284 (2008).

[15] See Supplemental Material at url://xxxx.

[16] A. Bercy, S. Guellati-Khelifa, F. Stefani, G. Santarelli, C. Chardonnet, P.-E. Pottie, O. Lopez, and A. Amy-Klein, J. Opt. Soc. Am. B **31**, 678 (2014), http://dx.doi.org/10.1364/JOSAB.31.000678.

[17] L. S. Ma, P. Jungner, J. Ye, and J. L. Hall, Opt. Lett. **19**, 1777 (1994), http://www.opticsinfobase.org/ol/abstract.cfm?URI=ol-19-21-1777.

[18] H. Jiang, F. Kéfélian, S. Crane, O. Lopez, M. Lours, J. Millo, D. Holleville, P. Lemonde, C. Chardonnet, A. Amy-Klein, and G. Santarelli, J. Opt. Soc. Am. B **25**, 2029 (2008).

[19] F. Stefani and *et al.*, (2014), in prep. ArXiv:2014/xxxx.

[20] S. Dawkins, J. McFerran, and A. Luiten, IEEE Trans. Ultrason. Ferroelectr. Freq. Control **54**, 918 (2007).

[21] S.-C. Ebenhag and P.-O. Hedvekist, **PTTI'11, Long Beach, Ca, 2011-11-14** (2011).

[22] W.-K. Lee, D.-H. Yu, C. Y. Park, and J. Mun, Metrologia **47**, 1394 (2010).

Supplemental Materials: Two-Way Optical Frequency Comparisons at $5 \cdot 10^{-21}$ relative stability Over 100-km Telecommunication Network Fibers

DESCRIPTION OF THE EXPERIMENTAL SET UP

The loop starts and ends at Laboratoire de Physique des Lasers and is constituted of six fibers spans (see Fig. SM1). In each span, we access two fibers placed in the same cable. Two non-consecutive spans of 10 km and 8 km are active telecommunication fibers from French Research Network (Renater), simultaneously used for data traffic. Eight OADMs are used to insert and to extract the ultra-stable signal at 1.5 μm into these spans. The four others spans are dedicated fibers. We installed halfway one Erbium-Doped Fiber Amplifier (EDFA) with 20 dB gain on each fiber to compensate partly the 45 dB losses measured on the first fiber. One additional EDFA was added on the second fiber to compensate extra-losses we observed on it.

The beat notes detected on photodiodes PD1 and PD2 are amplified and filtered. Those at frequency $f_1 + f_2$ are more attenuated because of a double circulation in the loop. Thus a tracking oscillator is phase locked to them with a bandwidth of 100 kHz. The resulting signals are simultaneously recorded with a gate time of 1 s with two dead-time free frequency counters (Kramer + Klische FXE) operated in Π-type and Λ-type.

ESTIMATE OF THE ACCURACY

We recorded the relevant beat notes with 1 s gate time and with Π-type counter, to avoid overweighting the center parts of the data sets with the triangular weighting of the Λ-type counter. Then we calculate the mean value of these frequencies and its standard deviation for consecutive segments from 1 to 1 000 s [S8]. For the bi-directional set up, with the set of 138 000 data of 1 s of Fig. 2, we obtained a mean offset frequency of $7 \cdot 10^{-21}$. The statistical relative uncertainty of the mean value, calculated as the relative standard deviation divided by the length of the consecutive segment, has a constant value of $3 \cdot 10^{-21}$ as expected for white phase noise [S22]. For longer segments, this value slightly increases, due to long-term Flicker noise. We finally set a conservative estimate of the statistical fractional uncertainty of the frequency comparison as the long-term overlapping Allan deviation of the data set, which is $2 \cdot 10^{-20}$ at 20 000 s integration time. For the two-way uni-directional, using 160 000 data of 1 s of the remote comparison, we find a relative mean offset frequency of $8 \cdot 10^{-18}$. We set the statistical fractional uncertainty of the frequency comparison as the long-term overlapping Allan deviation, that is $6.5 \cdot 10^{-17}$ at 40 000 s integration time.

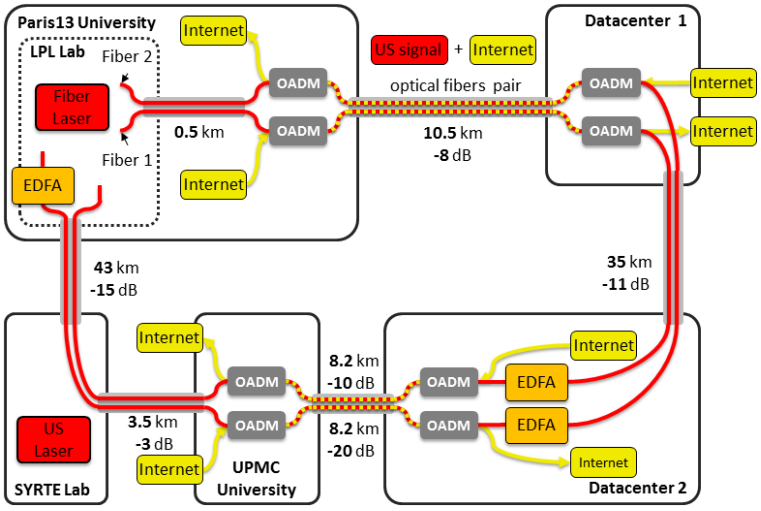

FIG. SM1. Sketch of the network infrastructure.

* paul-eric.pottie@obspm.fr

[S1] F. R. Giorgetta, W. C. Swann, L. C. Sinclair, E. Baumann, I. Coddington, and N. R. Newbury, Nat. Photon. **7**, 434 (2013), doi:10.1038/nphoton.2013.69.

[S2] B. J. Bloom, T. L. Nicholson, J. R. Williams, S. L. Campbell, M. Bishof, X. Zhang, W. Zhang, S. L. Bromley, and J. Ye, Nature **506**, 71 (2014), doi:10.1038/nature12941.

[S3] T. Kessler, C. Hagemann, C. Grebing, T. Legero, U. Sterr, F. Riehle, M. J. Martin, L. Chen, and J. Ye, Nat. Photon. **6**, 687 (2012), doi:10.1038/nphoton.2012.217.

[S4] M. Fujieda, D. Piester, T. Gotoh, J. Becker, M. Aida, and A. Bauch, Metrologia **51**, 253 (2014), doi:10.1088/0026-1394/51/3/253.

[S5] N. R. Newbury, P. A. Williams, and W. C. Swann, Opt. Lett. **32**, 3056 (2007), http://www.opticsinfobase.org/ol/abstract.cfm?URI=ol-32-21-3056.

[S6] K. Predehl, G. Grosche, S. M. F. Raupach, S. Droste, O. Terra, J. Alnis, T. Legero, T. W. Hänsch, T. Udem, R. Holzwarth, and H. Schnatz, Science **336**, 441 (2012), doi: 10.1126/science.1218442.

[S7] O. Lopez, A. Haboucha, B. Chanteau, C. Chardonnet, A. Amy-Klein, and G. Santarelli, Opt. Express **20**, 23518 (2012), http://dx.doi.org/10.1364/OE.20.023518.

[S8] S. Droste, F. Ozimek, T. Udem, K. Predehl, T. W. Hänsch, H. Schnatz, G. Grosche, and R. Holzwarth, Phys. Rev. Lett. **111**, 110801 (2013).

[S9] F. Kéfélian, O. Lopez, H. Jiang, C. Chardonnet, A. Amy-Klein, and G. Santarelli, Opt. Lett. **34**, 1573 (2009).

[S10] O. Lopez, A. Kanj, P.-E. Pottie, D. Rovera, J. Achkar, C. Chardonnet, A. Amy-Klein, and G. Santarelli, Applied Physics B **110**, 3 (2013).

[S11] D. W. Hanson, **Proc. of 43rd Annual Frequency Control Symposium** (1989).

[S12] G. G. S. D. S.M.F. Raupach, H. Schnatz, Proc. of European Frequency and Time Forum, (2012), dOI: 10.1109/EFTF.2012.6502357.

[S13] C. E. Calosso, E. Bertacco, D. Calonico, C. Clivati, G. A. Costanzo, M. Frittelli, F. Levi, A. Mura, and A. Godone, Opt. Lett. **39**, 1177 (2014), http://dx.doi.org/10.1364/OL.39.001177.

[S14] P. A. Williams, W. C. Swann, and N. R. Newbury, J. Opt. Soc. Am. B **25**, 1284 (2008).

[S15] See Supplemental Material at url://xxxx.

[S16] A. Bercy, S. Guellati-Khelifa, F. Stefani, G. Santarelli, C. Chardonnet, P.-E. Pottie, O. Lopez, and A. Amy-Klein, J. Opt. Soc. Am. B **31**, 678 (2014), http://dx.doi.org/10.1364/JOSAB.31.000678.

[S17] L. S. Ma, P. Jungner, J. Ye, and J. L. Hall, Opt. Lett. **19**, 1777 (1994), http://www.opticsinfobase.org/ol/abstract.cfm?URI=ol-19-21-1777.

[S18] H. Jiang, F. Kéfélian, S. Crane, O. Lopez, M. Lours, J. Millo, D. Holleville, P. Lemonde, C. Chardonnet, A. Amy-Klein, and G. Santarelli, J. Opt. Soc. Am. B **25**, 2029 (2008).

[S19] F. Stefani and *et al.*, (2014), in prep. ArXiv:2014/xxxx.

[S20] S. Dawkins, J. McFerran, and A. Luiten, IEEE Trans. Ultrason. Ferroelectr. Freq. Control **54**, 918 (2007).

[S21] S.-C. Ebenhag and P.-O. Hedvekist, **PTTI'11, Long Beach, Ca, 2011-11-14** (2011).

[S22] W.-K. Lee, D.-H. Yu, C. Y. Park, and J. Mun, Metrologia **47**, 1394 (2010).